Available online at www.sciencedirect.com
SCIENCE DIRECT®
Polymer 44 (2003) 6323–6333
polymer
www.elsevier.com/locate/polymer

Solubilities and diffusivities of water vapor in poly(methylmethacrylate), poly(2-hydroxyethylmethacrylate), poly(*N*-vinyl-2-pyrrolidone) and poly(acrylonitrile)

Oscar Rodríguez[a,b,1], Francesco Fornasiero[a,b], Alberto Arce[a,b,1], Clayton J. Radke[a,b], John M. Prausnitz[a,b,*]

[a]*Department of Chemical Engineering, University of California, Berkeley, CA, 94720-1462 USA*
[b]*Chemical Sciences and Earth Science Divisions, Lawrence Berkeley National Laboratory, Berkeley, CA 94720 USA*

Received 8 May 2003; accepted 15 July 2003

Abstract

Sorption and diffusion data were obtained for water vapor in four different polymers: poly (methylmethacrylate) (PMMA), poly (2-hydroxyethylmethacrylate) (PHEMA), poly (*N*-vinyl-2-pyrrolidone) (PVP) and poly (acrylonitrile) (PAN) at 35 °C using a gravimetric sorption method. Highest sorption was for PVP, followed by PHEMA. PMMA and PAN sorbed very little water. All the polymers exhibit a BET type III sorption isotherm; the large upturn at high activity for PVP and PHEMA is probably due to plasticization of the polymers by water vapor. Sorption data were interpreted using Flory–Huggins theory and the Zimm and Lundberg cluster integral.

Fickian diffusion is observed for PHEMA. For PVP, the fractional uptake M_t/M_∞ is linear with the square root of the time up to $M_t/M_\infty = 0.6 - 0.8$ for all water activities a_w, but it shows a clear water sorption overshoot at $a_w = 55.3\%$ and $a_w = 72.1\%$, probably due to macromolecular relaxation. PMMA sorption kinetics is also characterized by a maximum in the water uptake. The diffusion coefficient increases significantly with water concentration for PVP and PHEMA, weakly for PMMA, but it is independent of concentration for PAN.

Keywords: Water vapor sorption and diffusion; Clustering; Sorption overshoot

1. Introduction

Sorption and diffusion data are pertinent to a variety of applications including membrane separation of gases and vapors; packaging and coating technology; controlled drug-release systems, and biocompatible materials for biomedical applications. In particular, in the contact lens industry, recent efforts have been directed toward obtaining continuous-wear lenses, i.e. lenses that can be worn for up to 1 month without removal from the eye [1]. For a successful product, the lens must provide both appreciable water content and oxygen permeability. Comfort and on-eye movement correlate with water content and water transport through hydrogel contact lenses [2–4].

Because of its practical importance, water as penetrant has received increasing attention in recent studies of vapor-sorption and diffusion in polymeric materials [5–18]. Water is a complex penetrant because, due to its polarity and ability to form hydrogen bonds, it may interact strongly with itself or with the polymer. Water also has a tendency to cluster and to cause plasticization of the polymer matrix [18].

When a penetrant diffuses into a polymer film, the macromolecules rearrange toward a new configuration with a relaxation rate that depends on temperature as well as on solvent concentration. The relative time scales of the diffusion and relaxation processes determine the nature of the transport process. Vrentas et al. [19] defined a diffusive Deborah number *De* as the ratio of the characteristic relaxation time λ and the diffusion time, L^2/D, where D is the diffusion coefficient and L is the film thickness. For $De \ll 1$ the diffusion rate is significantly slower than the relaxation rate of the polymer chain, and Fickian diffusion is observed. Fujita [20] has summarized the characteristic

* Corresponding author. Tel.: +510-642-3592; fax: +510-642-4778.
E-mail address: prausnit@cchem.berkeley.edu (J.M. Prausnitz).
[1] Present address: Department of Chemical Engineering, University of Santiago de Compostela, Spain.

0032-3861/$ - see front matter © 2003 Published by Elsevier Ltd.
doi:10.1016/S0032-3861(03)00654-2

features of Fickian sorption of a solvent in a polymer film (slab geometry), suddenly exposed to an environment at constant solvent activity. If the surface concentration in the polymer instantaneously reaches the equilibrium value, (i) a plot of the fractional penetrant uptake M_t/M_∞ (where M_t is the mass of penetrant absorbed at time t, and M_∞ the equilibrium one) versus the square root of the time is linear up to $M_t/M_\infty = 60\%$ (or more) for both absorption and desorption; (ii) beyond the linear portions, both sorption curves are concave to the time axis, independent of the form of the concentration dependence of D; (iii) a series of absorption curves between the same initial and final solvent concentrations in films of different thicknesses gives superposable plots of M_t/M_∞ versus $t^{0.5}/L$. When the time scales of diffusion and relaxation are of comparable magnitude ($De \sim 1$), a series of anomalous features may be encountered in the kinetic sorption curve; any of the conditions (i)–(iii) may be violated. Therefore, Fickian behavior is expected for rubbery polymers at temperatures well above the glass-transition temperature, whereas anomalous sorption is more likely to occur for polymer–penetrant mixtures in the glassy state.

The most commonly used method to characterize the nature of the transport process is to fit the initial portion of the sorption curve with

$$\frac{M_t}{M_\infty} = kt^\alpha. \tag{1}$$

For a flat sheet, anomalous diffusion is indicated by $0.5 < \alpha < 1$, while $\alpha = 0.5$ corresponds to Fickian diffusion [21]. However, many factors other than the polymer relaxation may produce anomalous features including a non-planar geometry, time-dependent surface concentrations or anisotropic dimensional changes in the polymer sample, even if the rate-controlling process is Fickian at the molecular level [22]. Anomalous α values, therefore, may not be specifically connected with polymer relaxation.

This work concerns solubility and diffusion of water vapor in four homopolymer films whose monomers are commonly used in formulations for contact lenses. We report experimental data for water vapor sorption and water diffusion through polymer films at 35 °C, the average temperature of a contact lens on the eye [23]. Water clustering, polymer plasticization, and the nature of the diffusion process are discussed. The data reported here are of interest for the development of packaging and insulation materials and for design of continuous-wear contact lenses, in addition to other biomedical applications.

2. Experimental section

2.1. Materials

Water is obtained from a Barnstead NANOpure® system and degassed with a standard freeze/thaw procedure. Polymers used are poly (2-hydroxyethyl methacrylate) (PHEMA), poly (methyl methacrylate) (PMMA), poly (*N*-vinyl-2-pyrrolidone) (PVP), and poly (acrylonitrile) (PAN).

Table 1 gives characteristics of the four polymers: supplier, CAS-register number, molecular weight, density, glass-transition temperature, solvent and drying temperature used for film casting. The glass-transition temperature of each polymer was measured by modulated differential scanning calorimetry (DSC 2920, Modulated DSC, TA Instruments). Solvents used are methanol (EM Science, 99.8%), chloroform (Fisher Scientific, 99.9%, with 0.8 v/v% ethanol as preservative) and dimethyl sulfoxide (DMSO) (Fisher Scientific, 99.9%). Details are available elsewhere [24].

2.2. Procedure

Polymer films are prepared by solvent casting using the solvents shown in Table 1. Each film is dried at a temperature higher than its glass-transition temperature (Table 1) for 24 h to remove the solvent completely. The film is then cooled slowly (0.2 °C/min) in a vacuum oven (Napco E series model 5851) flushed with dry N_2. Except for water-soluble PVP, the films are pre-equilibrated with liquid water for 24 h and then dried following the same procedure to standardize their histories. The dry-film thickness is measured using a micrometer (Mitutoyo MDC 0-1' PF, accuracy ± 3 μm) at different locations; the average (reported in Table 3 with the standard deviation) is used for subsequent calculations.

A gravimetric sorption method is used for both sorption and diffusion experiments. Fig. 1 shows a schematic of the apparatus. The measured elongation of a calibrated quartz

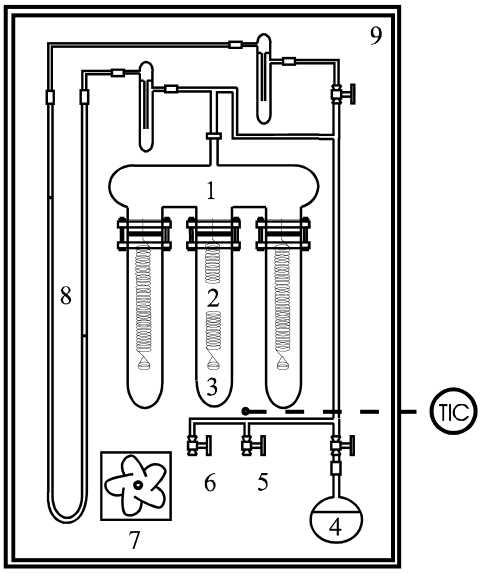

Fig. 1. Schematic of the apparatus for water vapor sorption and diffusion measurements: (1) glass chamber, (2) quartz spring, (3) quartz pan, (4) solvent flask, (5) vacuum line, (6) vent, (7) fan, (8) 1-octadecene manometer, (9) air thermostatic bath.

Table 1
Polymer properties

Polymer	Supplier	CAS No.	M.W.	Density[a] (g/ml)	T_g (°C)	Solvent	T_{drying} (°C)
PHEMA	Polysciences	25249-16-5	200,000	1.15	121	Methanol	145
PMMA	SP2	9011-14-7	540,000	1.2	119	Chloroform	145
PVP	SP2	9003-39-8	360,000	1.16[b]	181	Water	210
PAN	SP2	25014-41-9	150,000	1.184	85[a]	DMSO	145

SP2: Scientific Polymer Products, Inc.
[a] Indicated by Scientific Polymer Products, Inc. Our DSC experiments do not show a clear glass-transition for PAN.
[b] Kaplan and Guner [56].

spring (Ruska Instruments) determines the water uptake in the polymer. Springs are calibrated using known masses previously weighed with a Mettler M3 microbalance to a precision of ± 1 μg; the springs have a sensitivity of about 5 mm/mg. The calibration curves are linear in all cases. Elongation measurements are corrected for the temperature-dilation effect as suggested by Ruska:

$$L_C = L_M[1 + 1.35 \times 10^{-4}(T - T_0)], \quad (2)$$

where L_C and L_M are, respectively, the corrected and measured lengths and T and T_0 (in °C) are, respectively, the experimental and calibration temperatures.

A U-tube manometer is used to measure the pressure. The manometer liquid is 1-octadecene, selected because of its low vapor pressure, immiscibility with water, and suitable density for the pressure range of interest here. The density of 1-octadecene is calculated with an equation from Daubert and Danner [25].

Spring elongation and manometer-liquid height difference are measured with a cathetometer (Wild, model KM274) with a precision of ± 0.1 mm. The glass apparatus is enclosed in an air bath with an Omega CN9000 PID controller (accuracy ± 0.5 °C) to maintain the experimental temperature very close to 35 °C.

2.3. Vapor-sorption equilibria

For each run, polymer samples (~ 10–25 mg) are attached to three springs. If the polymer is hydrophilic, it is loaded onto a quartz pan (~ 10 mg); if it is hydrophobic, it is directly attached to the spring hook. After closing the glass chambers, the apparatus is evacuated with the vacuum pump, and both the manometer liquid and the water are degassed by a standard freeze/thaw procedure [26]. The polymers are dried at 80 °C for at least 24 h until a constant weight is achieved. Then the temperature is set to 35 °C, and a vacuum test is carried out to ensure that the apparatus can maintain the desired pressure (changes of less than 0.3 Torr/day).

When the vacuum test is successful, water vapor is injected by opening the solvent flask valve. Spring elongation and pressure are measured at several time steps until equilibrium is reached (20–40 h), i.e. when a few successive measurements agree to within experimental error. Then a new water injection is made. The experiments correspond to a range of vapor activities, a_w, from 15 to 90%. Water activity is calculated assuming an ideal gas phase of pure water vapor, i.e. neglecting the vapor pressure of 1-octadecene and of the polymer:

$$a_w = \frac{p}{p_w^0}, \quad (3)$$

where p is the pressure and p_w^0 is the water saturation pressure taken from Daubert and Danner [25].

2.4. Diffusion

In this case, only one sample is used at a time. Preparation steps are identical to those for the equilibrium-sorption experiment: spring calibration, degassing of 1-octadecene and water, drying of the polymer sample, and vacuum test. Following vapor injection, the water uptake and time are measured simultaneously. Time is obtained from a stopwatch (Fisher Scientific, uncertainty = 0.13 s), started as soon as the manometer liquid moves. Measurements are repeated until equilibrium is attained. After equilibration, the polymer is dried as described above. The diffusion experiments are performed by suddenly raising water vapor activity from 0 to 20, 40, 60 or 80% (integral sorption).

3. Results and discussion

3.1. Vapor-sorption equilibria

Fig. 2 gives the vapor-sorption equilibrium data. Water weight fraction in the polymer is plotted against water vapor activity calculated from Eq. (3). Due to their hydrophobic character, PMMA and PAN absorb only small amounts of water (roughly 2 wt% at the highest activity). Stannett et al. [27] reported a slightly higher sorption for PAN at all activities; the sorption curve obtained by Katchman and McLaren [28] at 25 °C overlaps our results for $a_w < 0.6$, but it departs significantly from our and Stannett's measurements at highest water activities. The measured water uptake in PMMA agrees well with previous reports [29].

Water sorption in water-soluble PVP is the largest and is

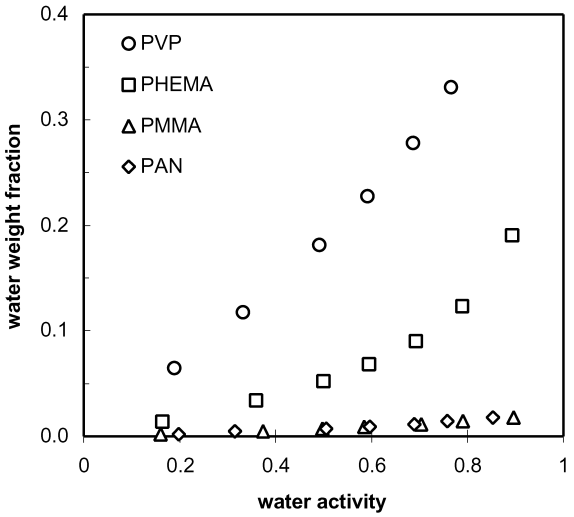

Fig. 2. Water vapor sorption equilibria for PVP, PHEMA, PMMA and PAN at 35 °C.

in good agreement with previous data [13]. The sorption curve for PHEMA lies between those for PVP and the hydrophobic polymers, as expected because PHEMA swells in liquid water but it does not dissolve. Our PHEMA sorption measurements compare favorably with recent literature data for water vapor at 37 °C [30].

The polymers considered here have glass-transition temperatures T_g in the dry state higher than the experimental temperature (see Table 1). However, a water weight fraction of roughly 8% [30] and 17–21% [31–33] lowers T_g of PHEMA and PVP, respectively, to 35 °C. Therefore, a change from the glassy to the rubbery state occurs for both PVP and PHEMA at high activity. For PMMA and PAN, we can estimate the required water content to produce a glass-transition at 35 °C by applying the Flory–Fox equation [34]:

$$\frac{1}{T_{gm}} = \frac{w_w}{T_{gw}} + \frac{w_p}{T_{gp}}, \tag{4}$$

where w is the weight fraction, and subscripts w, p and m indicate water, polymer, and mixture, respectively. T_{gw} is equal to −135 °C [15,32,33]. The estimated water weight fractions are 15 and 10%, for PMMA and PAN respectively. These values are much higher than the maximum water sorbed in our experiments. Consequently, PMMA and PAN remain in the glassy state over the entire measured range of water activity.

To assess the strength of polymer–water interaction, we adopt Flory–Huggins theory [35] to correlate the sorption isotherms:

$$\ln a_w = \ln \Phi_w + \left(1 - \frac{1}{r}\right)\Phi_p + \chi\Phi_p^2, \tag{5}$$

where Φ_w and Φ_p are the water and polymer volume fractions, r is the number of segments in the polymer molecule, and χ is the Flory solvent–polymer interaction parameter. Because Flory–Huggins theory strictly applies only to rubbery polymers, our interaction parameters are 'effective' parameters when the polymer–solvent mixture is glassy. Fig. 3 displays χ as a function of water vapor activity for the four polymers. The χ value provides a good (inverse) indication of the solvent power of the penetrant (water) for the polymers [36]: water is a good solvent for PVP ($\chi \cong 0$) and a non-solvent for PHEMA, PMMA, and PAN ($\chi > 1$). For PHEMA χ is very close to 1, borderline for solvent character. Fig. 3 indicates that χ is concentration-dependent for all polymers, increasing with water activity for PVP but decreasing for PHEMA, PMMA, and PAN.

According to the BET classification [37], all the polymers exhibit a type III isotherm (Fig. 2), although the small sorptions in PMMA and PAN do not show this clearly, unless the water weight fraction axis in Fig. 2 is enlarged. Results for PVP and PHEMA portray a large upturn at high activity, whereas the upturn is less pronounced for PMMA and PAN.

Two possible explanations for a large degree of upturn at high activity are clustering of water molecules or plasticization of the polymer matrix induced by water sorption [15]. We consider plasticization at the end of the diffusion section. The Zimm and Lundberg cluster integral [38] provides a method to determine the extent of clustering of the solvent molecules inside the polymer matrix. The advantage of this integral is that it can be obtained directly from equilibrium data using the following relation:

$$\frac{G_{ww}}{v_w} = -\Phi_p\left[\frac{\partial\left(\frac{a_w}{\Phi_w}\right)}{\partial a_w}\right]_{P,T} - 1, \tag{6}$$

where G_{ww} is the cluster integral, v_w is the partial molecular volume, both for the water molecules. The quantity G_{ww}/v_w gauges the tendency of sorbed molecules to cluster. If $G_{ww}/v_w = -1$, the solution is ideal: water molecules exclude their own volumes to the other water molecules

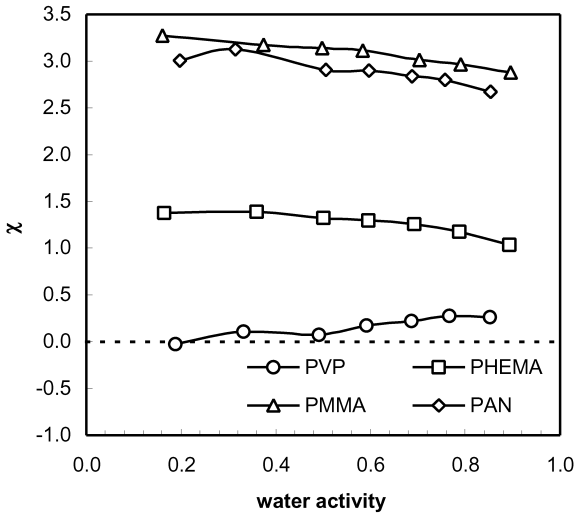

Fig. 3. Flory interaction parameter χ versus water vapor activity for PVP, PHEMA, PMMA and PAN at 35 °C.

but have no other effect on their distribution. $G_{ww}/v_w = 0$ means that clustering is just sufficient to overcome the excluding effect of the central water molecule, whereas $G_{ww}/v_w > 0$ indicates that the water molecules tend to cluster. If $G_{ww}/v_w < -1$, the water molecules prefer to remain isolated.

Fig. 4a compares the values of the clustering function G_{ww}/v_w for the four polymers. To calculate G_{ww}/v_w, we first fit our experimental equilibrium data (Φ_w versus a_w) with Eq. (5), where we assume $\chi = c_1\Phi_w + c_2$ with c_1 and c_2 constants. We then differentiate the resulting smooth function. Although the calculated values may vary somewhat with differing smoothing procedures, the following conclusions remain valid. Results for PVP give a small negative G_{ww}/v_w for water activities up to 0.76, whereas at very high activity, G_{ww}/v_w becomes slightly positive, suggesting that water does not cluster in this polymer. Conversely PHEMA, PMMA and PAN exhibit positive values for G_{ww}/v_w, indicating that water molecules tend to cluster in these polymers, as expected for poor solvents [36]. The clustering tendency increases significantly in the order PMMA > PAN > PHEMA > PVP.

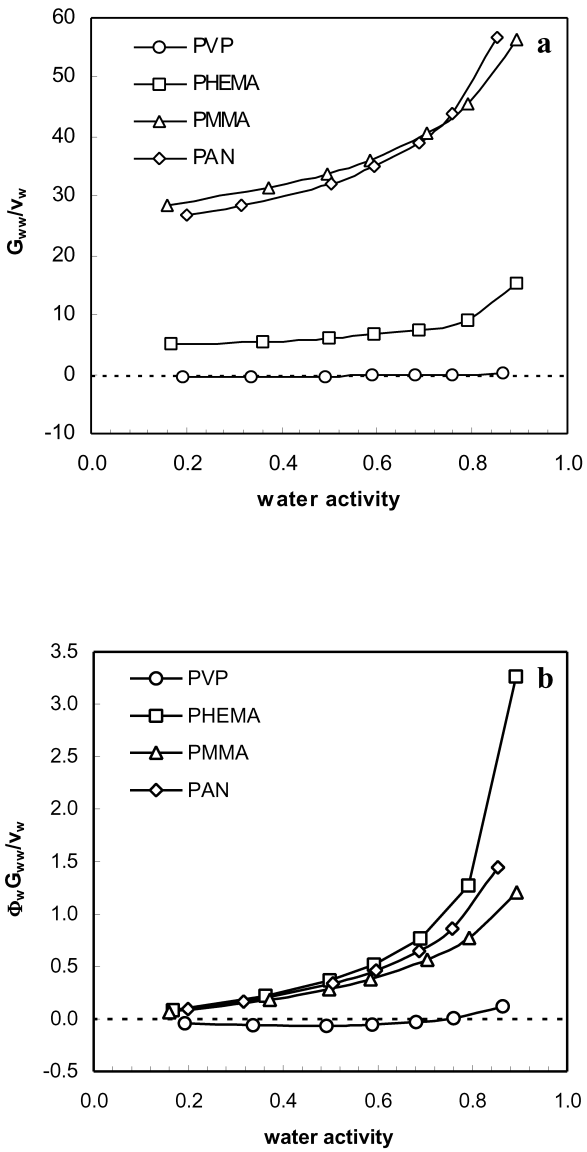

Fig. 4. Clustering function G_{ww}/v_w (a) and mean cluster size $\Phi_w G_{ww}/v_w$ (b) at various water vapor activities for PVP, PHEMA, PMMA and PAN at 35 °C.

The product $\Phi_w G_{ww}/v_w$ represents the mean number of water molecules in excess of the mean water concentration in the specific neighborhood of a given water molecule [38]. Fig. 4b shows the mean cluster size, $\Phi_w G_{ww}/v_w$, as a function of water vapor activity for the four polymers. For PVP, $\Phi_w G_{ww}/v_w$ is small and negative (> -0.1), in good agreement with data from Chang et al. [13], except at very high activity, where it becomes slightly positive. PHEMA, PMMA and PAN display positive values increasing with water activity, indicating that clusters of larger size form at high activity. Stannett et al. [39] and Ranade et al. [40] reported a similar range of values for PAN for $a_w > 0.5$, whereas at lower a_w values their sorption curves are concave to the activity axis suggesting no clustering.

Our results obtained for χ and G_{ww}/v_w indicate a large difference for water interacting with the four polymers. When the polymer–water interaction is strong (PVP), water is a good solvent for the polymer, and water molecules do not cluster in the polymer matrix. By contrast, upon reducing the polymer–solvent affinity (larger χ), the solubility of water decreases, and water tends to cluster in the polymer matrix (larger G_{ww}/v_w).

3.2. Fickian versus anomalous diffusion

A change from the glassy to the rubbery state occurs for both PVP and PHEMA at high water activity, whereas PMMA and PAN remain in the glassy state at all activities. Therefore, anomalous diffusive behavior is expected for our systems. To understand the nature of the diffusion process in our polymers, we fit the exponent α in Eq. (1) to our experimental data. Table 2 summarizes the results. For PAN, α is very close to 0.5 at all activities, suggesting Fickian diffusion. Too few data have been collected for PMMA at short time for an accurate determination of α. For PHEMA ($L = 302$ μm), a plot of $\ln(M_t/M_\infty)$ versus $\ln t$ fails to show a linear relationship for some activities (see example in Fig. 5a). When the linear relationship holds, the fitted α is inside the range of anomalous diffusion ($\alpha = 0.58 - 0.62$). However, if we plot M_t/M_∞ versus $t^{0.5}/L$, an excellent linear correlation ($R^2 > 0.995$, most often ~ 0.999) is found for M_t/M_∞ up to 60–75% at all activities. However, the linear fit produces a nonzero intercept with the time axis (Fig. 5b). This suggests that after a short time lag, the diffusion process follows Fickian kinetics. The time lag in our data probably follows from an unavoidable experimental artifact: it is not possible to raise instantaneously solvent activity and surface concentration to the equilibrium value. We collect the time data starting from the instant when the manometer liquid begins to move. Some

Table 2
Exponent α in Eq. (1) for varying water activities

Polymer[a]	a_w	α	R^{2b}
PVP	0.187	0.57	0.9987
	0.384	0.65	0.9987
	0.550	0.72	0.9998
	0.721	0.77	0.9983
PHEMA	0.181	–	–
$L = 181$ μm	0.368	0.69	0.9818
	0.598	0.65	0.9959
	0.776	0.72	0.9974
PHEMA	0.192	–	–
$L = 302$ μm	0.379	–	–
	0.598	0.58	0.9991
	0.761	0.66	0.9958
PAN	0.394	0.46	0.9365
	0.571	0.51	0.9818
	0.747	0.47	0.9926

[a] For PMMA too few data have been collected at short times for an accurate determination of α.
[b] R^2 is the square of the correlation coefficient.

time is needed before the system attains the desired solvent activity and equilibrium with the solvent surface. As a consequence, a sigmoidal shape of the sorption curve is expected at the very early stage of the sorption [41]; this sigmoidal shape appears as a time lag in the uptake kinetics because we start to collect data a few minutes after water injection.

To verify the Fickian nature of the water transport in PHEMA, we performed a second set of diffusion experiments for the same range of solvent activities with a film of different thickness ($L = 181$ μm). In spite of the short delay discussed above, the sorption curves for different thicknesses are superposable at all activities, as shown in Fig. 6 for the two extreme activities. We conclude that water sorption in PHEMA is Fickian. Our results are supported by the studies of Gehrke et al. [22] who documented Fickian water transport in originally glassy PHEMA. Therefore, anomalous α values may simply arise from a delay in raising the penetrant surface concentration to the equilibrium value, and not from polymer relaxation.

For PVP, α rises from 0.57 to 0.77 upon increasing water activity. The plot $\ln(M_t/M_\infty)$ versus $\ln t$ shows an excellent linear relationship for all activities (see Fig. 5a for $a_w = 0.187$). However, a plot M_t/M_∞ versus $t^{0.5}/L$ also shows very good linear correlation, especially at low activities, with a nonzero intercept (Fig. 5b). Based on the previous discussion, either a time lag or polymer relaxation may be a source of an anomalous α. Occurrence of a sorption overshoot, discussed in Section 3.3, caused by polymer relaxation suggests that relaxation is important in PVP.

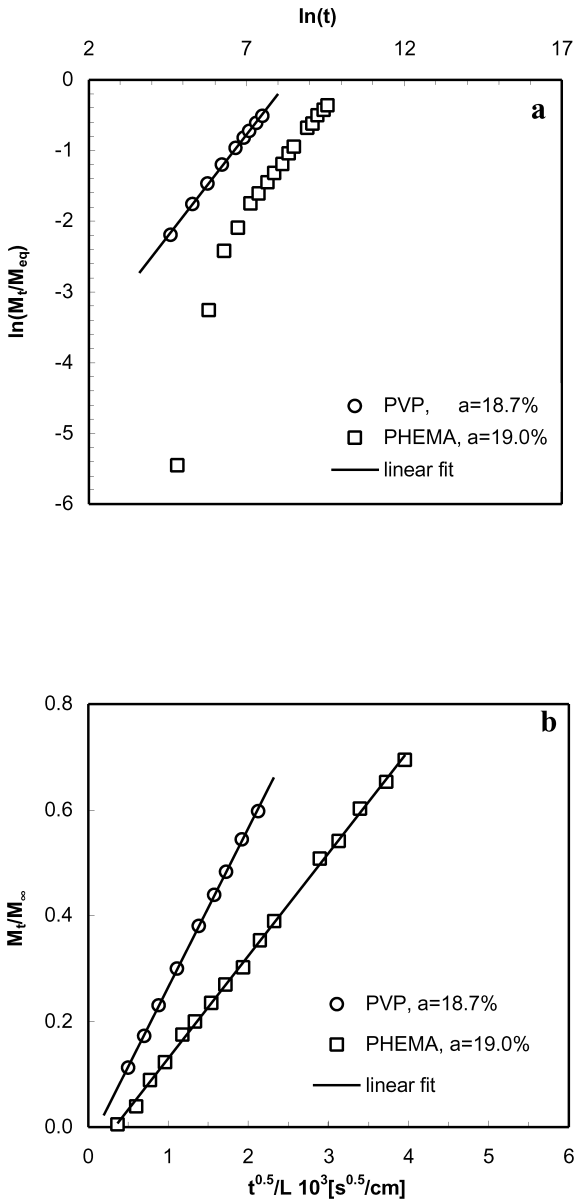

Fig. 5. Water uptake at early time for PVP ($a_w = 18.7\%$) and PHEMA ($a_w = 19.0\%$, $L = 302$ μm) (a) in $\ln(M_t/M_\infty)$ versus $\ln t(s)$ plot, and (b) in M_t/M_∞ versus $t^{0.5}/L$ plot.

3.3. Sorption overshoot

A plot of the fractional penetrant uptake M_t/M_∞ versus $t^{0.5}/L$ for PVP and PMMA at high activities (0.55 and 0.72 for PVP; 0.55 and 0.82 for PMMA, respectively) in Fig. 7 presents a characteristic maximum before reaching the equilibrium value. This feature of uptake kinetics, called 'sorption overshoot', is in general due to a rearrangement of the polymer chains following plasticization induced by a penetrant.

Four possible causes of sorption overshoot are reported in the literature. First, sorption overshoots are observed when the absorption of a fluid in crystallizable glassy or rubbery polymers promotes crystallization [42,43]. Solvent-

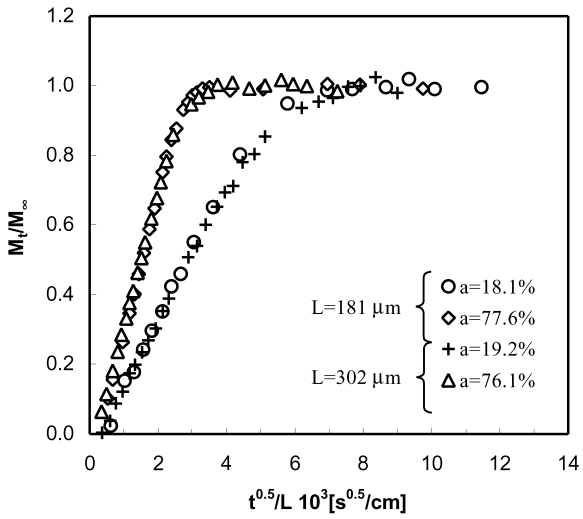

Fig. 6. Comparison of the fractional uptake versus the ratio of square root of time to film thickness for PHEMA with two different thicknesses at two activities and 35 °C.

induced crystallization (SINC) can be detected from the appearance of a characteristic kink in the equilibrium sorption curve, by a reduction in the equilibrium uptake in a second sorption run, or by testing the polymer sample for change in crystallinity before and after sorption.

Second, a penetrant-induced melting of labile crystals and subsequent formation of stable crystals may lead to a sorption-uptake maximum without a net change in the crystallinity fraction and, therefore, in the equilibrium uptake [44]. Penetrant-induced melting and recrystallization can be verified by modulated differential scanning calorimetry (MDSC).

Third, sorption overshoot in rubbery [45–48] or glassy [49] polymers may arise from a slow relaxation of the polymer chains to a more compact structure. In this case, there is no crystallinity after sorption, and the solvent equilibrium-uptake in two consecutive sorption runs is unchanged.

Finally, a maximum in kinetic sorption curve may be caused by release of indigenous components of the polymer matrix after contact with a liquid [50,51].

We exclude this last possibility because, during the experiment, the polymer films contact solvent vapor and not liquid, and because the films were soaked in liquid water and subsequently dried before any uptake experiment. This procedure eliminates any water-soluble or volatile component before collecting sorption data. Moreover, the weight of the dry polymer sample was unchanged after each desorption step.

No kink is present in our equilibrium-sorption data (see Fig. 2), suggesting that there is probably no significant solvent-induced crystallization in our samples. For a crystallizable polymer, the pre-equilibration step with liquid water promotes the formation of crystals. Therefore, it is unlikely that crystallization (SINC or solvent-induced melting and recrystallization) occurs in the subsequent water vapor sorption at activities lower than unity. Hence, the observed overshoot is most likely caused by polymer relaxation.

However, to distinguish between a process involving crystallization and a simple polymer relaxation, we performed a calorimetric analysis on our samples after pre-equilibration with liquid water. No melting peak was detected for any of the four polymers studied upon heating to 400 °C. Consequently we conclude that PVP, PMMA do not crystallize after water sorption and, therefore, that the sorption kinetic overshoot is due to polymer relaxation.

Sorption overshoot is observed if the diffusion time scale is smaller than the time scale for polymer-chain rearrangement (relaxation or crystallization). Indeed, the degree of overshoot, defined as

$$\frac{M_{\max} - M_\infty}{M_\infty} \tag{7}$$

decreases when the diffusion rate is reduced compared with the polymer relaxation rate, for example, by increasing the film thickness [42] or by lowering the temperature [43], by increasing the degree of polymer crosslinking or by using penetrants of larger size [49,52]. It is also well known that the maximum in solvent uptake is more pronounced at high solvent activities where the rate of penetrant diffusion in the polymer is faster [45,46].

We observe this behavior in our experimental data. PVP sorption curves do not show any evidence of overshoot at the lowest activities ($a_w = 18.7\%$ and $a_w = 38.4\%$), whereas a maximum in the solvent uptake appears at $a_w = 55.0\%$ (Fig. 7a); the maximum becomes more pronounced at $a_w = 72.1\%$ with a degree of overshoot of 4.5% (Fig. 7b). Similar behavior is observed for PMMA films in Fig. 7c and d. The degree of overshoot for PMMA is roughly 2% at $a_w = 55.3\%$ and 4% at $a_w = 82.1\%$.

3.4. Diffusion model

To interpret our data we require a model that is able to describe the variety of behaviors observed in our experiments: Fickian diffusion with time lag (PHEMA) and without time lag (PAN) as well as possible anomalous diffusion (PVP). Long and Richman [53] proposed a variable surface-concentration model to describe an anomalous, sigmoidal sorption curve. Although the transport process in the film is assumed to be Fickian, a non-instantaneous equilibration at the film surface is responsible for the anomalous feature. We interpret our data using a simplified version of Long and Richman's variable-surface-concentration model, suggested by Crank [41]. We assume that the diffusion process is Fickian, and that the water surface concentration approaches exponentially the equilibrium water concentration, C_0, at the selected activity:

$$C(\pm l, t) = C_0[1 - \exp(-\beta t)], \tag{8}$$

where $l = L/2$ and β is the inverse of the characteristic time

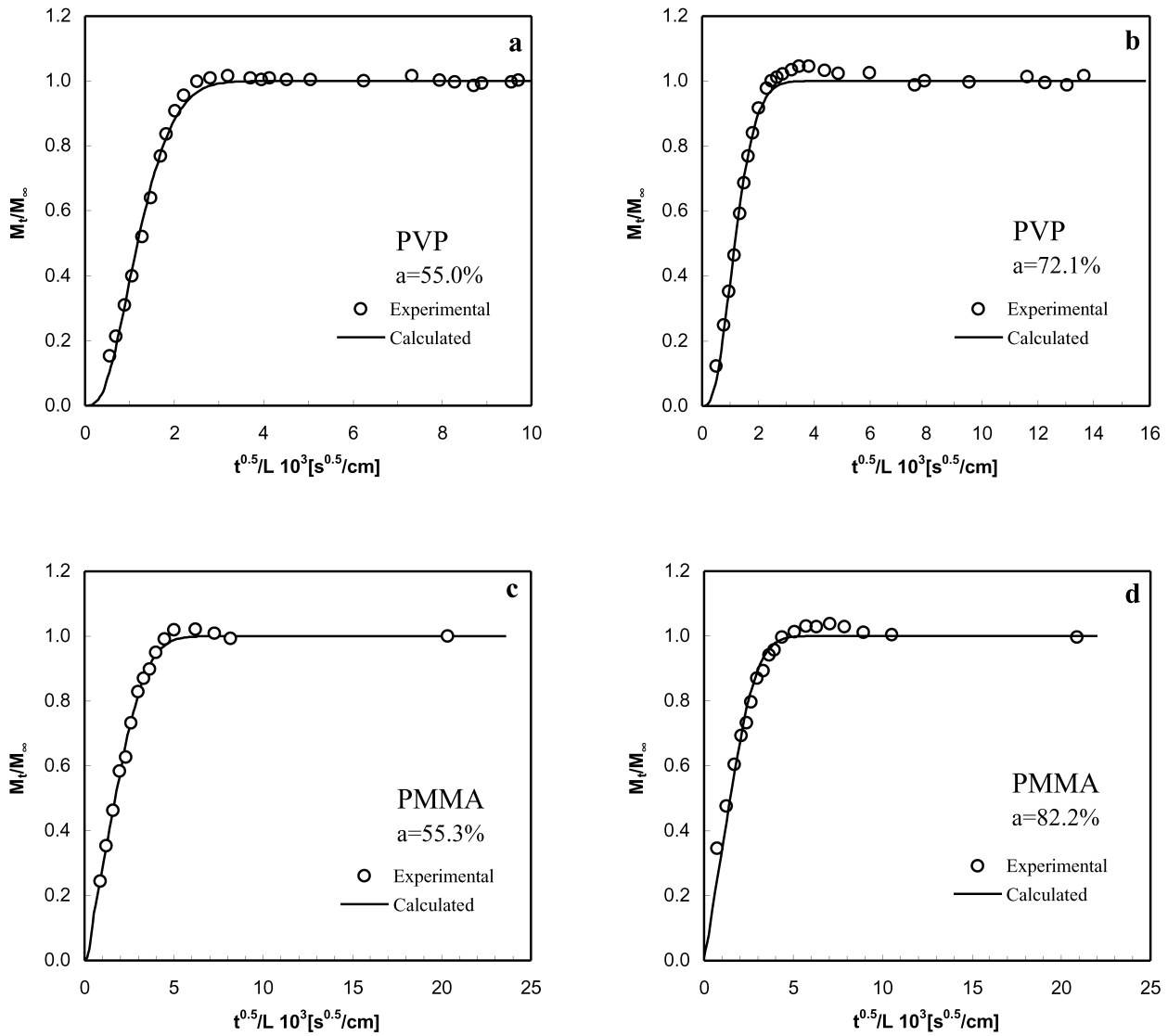

Fig. 7. Sorption overshoot in PVP at (a) $a_w = 55.0\%$ and (b) $a_w = 72.1\%$, and in PMMA at (c) $a_w = 55.3\%$ and (d) $a_w = 82.2\%$. Points are experimental data; lines are fitting curves using Eq. (9).

for attaining saturation at the surface. If this characteristic time is short, but not negligible, compared with the diffusion time scale, the predicted sorption curve has Fickian scaling ($\alpha = 0.5$) after a short delay.

The solution of Fick's second law with the boundary condition given by Eq. (8) and with a constant diffusion coefficient D is [41]:

$$\frac{M_t}{M_\infty} = 1 - \exp(-\beta t)\left(\frac{D}{\beta l^2}\right)^{1/2} \tan\left(\frac{\beta l^2}{D}\right)^{1/2} - \frac{8}{\pi^2}\sum_{n=0}^{\infty} \frac{\exp\left[-D(2n+1)^2\pi^2\frac{t}{4l^2}\right]}{(2n+1)^2\left\{1-(2n+1)^2\left[\frac{D\pi^2}{\beta 4l^2}\right]\right\}}. \quad (9)$$

In the limit of $\beta \to \infty$ (no time lag), we recover the typical Fickian curve for constant surface concentration, constant diffusion coefficient, and constant temperature. Eq. (9) cannot describe sorption overshoot. However, it is reasonable to adopt Eq. (9) to fit diffusion coefficients to sorption curves displaying overshoot, since the overshoot occurs near the end of the diffusion process. This is because the sorption maximum appears only if penetrant diffusion is faster than polymer relaxation. Moreover, the degree of kinetic overshoot for both PMMA and PVP is small.

Fig. 8 shows water-sorption kinetics in four polymers for different penetrant activities. Points are experimental data, whereas lines represent the fitting curves obtained with Eq. (9). The fit is satisfactory for all polymers at each activity. Table 3 shows the fitted diffusion coefficient D and β at each activity together with the root mean square deviation of the calculated water uptake and the film thickness for each polymer. We used the SigmaPlot© program with a least-squares method to calculate D and β from Eq. (9). In

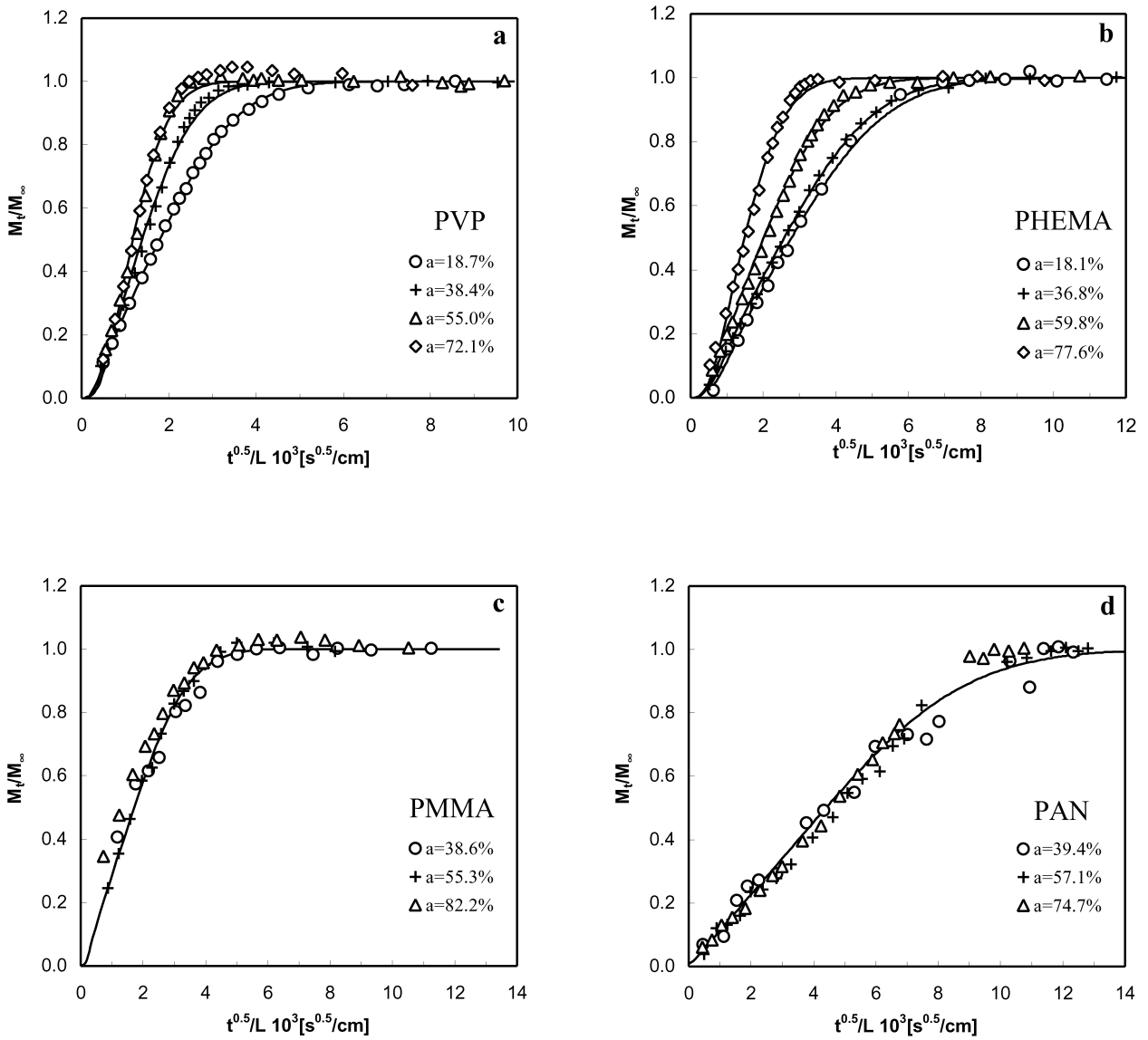

Fig. 8. Comparison of the fractional uptake versus the ratio of square root of time to film thickness for (a) PVP, (b) PHEMA ($L = 302$ μm), (c) PMMA and (d) PAN at several activities and 35 °C. Points are the experimental data, lines the fitting curves using Eq. (9). For clarity of presentation, the fitting curve is shown only at one activity for PMMA ($a_w = 55.3\%$) and PAN ($a_w = 74.7\%$), whereas for PVP that one at $a_w = 72.1\%$ is omitted.

general, the diffusion coefficient is concentration dependent; thus, the diffusion coefficients reported here are averages for a concentration range from zero to the equilibrium value at a given indicated activity.

The inverse of β measures the characteristic time required to reach the equilibrium water content at the sample surface, including the time necessary to raise the vapor activity to the desired level. Typical values of $1/\beta$ are in the range 0.5–6 min for PVP and PHEMA, whereas $1/\beta$ is close to zero for PAN and PMMA (within experimental uncertainty). In all cases $1/\beta$ is much smaller than the diffusion time scale, i.e. $(1/\beta)/(l^2/D) \ll 1$.

The water diffusion coefficient is concentration independent in PAN within the experimental uncertainty ($D \cong 2.4 \times 10^{-9}$ cm^2/s). Stannett et al. [27] reported diffusion coefficients for water in PAN ($D = 2.5–4 \times 10^{-10}$ cm^2/s at 30 °C and $4–10 \times 10^{-10} \times$ cm^2/s at 45 °C) smaller than our values, displaying a maximum with water concentration. Because PAN is glassy at these experimental temperatures, differences in the sample thermal history may account for the discrepancy between our results and those of Stannett.

For PMMA, D increases slightly at high activities (from 16×10^{-9} to 23×10^{-9} cm^2/s). Within the activity range studied here, the diffusion coefficient always increases with rising water vapor activity for PVP and PHEMA. For the former D is between 16×10^{-9} and 61×10^{-9} cm^2/s, and for the latter, D is between 6.9×10^{-9} and 31×10^{-9} cm^2/s. Ichikawa et al. [54] obtained similar values for D ($12.3–16.8 \times 10^{-9}$ cm^2/s) in PMMA and in PHEMA ($7.1–8.9 \times 10^{-9}$ cm^2/s) at $a_w = 50\%$. Our measured diffusion coefficient for water in PVP falls in between those reported

Table 3
Fitted diffusion coefficients (D) and time scale for variation of surface concentration ($1/\beta$) at water activity a_w, for PVP, PHEMA, PMMA, and PAN films with thickness L

Polymer	L (μm)	a_w	($D \times 10^9$ cm^2/s)	$1/\beta$ (s)	rmsd%[a]
PVP	$L = 202 \pm 4$ μm	0.187	16	40	0.13
		0.384	30	112	0.75
		0.550	55	138	1.01
		0.721	61	195	0.91
PHEMA	$L = 181 \pm 6$ μm	0.181	6.9	208	0.36
		0.368	7.9	142	0.15
		0.598	14	147	0.51
		0.776	31	187	0.90
PHEMA	$L = 302 \pm 5$ μm	0.192	6.4	453	0.13
		0.379	6.9	350	0.15
		0.598	13	270	0.68
		0.761	26	208	0.58
PMMA	$L = 106 \pm 2$ μm	0.386	16	0	1.88
		0.553	17	6	0.11
		0.821	23	0	2.35
PAN	$L = 238 \pm 8$ μm	0.394	2.4	0	0.49
		0.571	2.2	33	0.11
		0.747	2.5	0	0.27

[a] rmsd% is the root-mean-square deviation between the experimental and the calculated water uptakes.

by Ichikawa et al. [54] ($7.4–11.8 \times 10^{-9}$ cm^2/s) and Chang et al. [13] ($7–10 \times 10^{-8}$ cm^2/s).

The Fickian diffusion coefficient $Đ$ for a binary system can be written as the product of two terms [55]; the first one is an intrinsic mobility, $Đ$ while the second one is a thermodynamic non-ideality factor, Γ, defined by

$$\Gamma = \frac{\partial \ln(a_w)}{\partial \ln(\Phi_w)}. \quad (10)$$

Fig. 9 shows the thermodynamic factor for our systems calculated from the measured equilibrium water uptake.

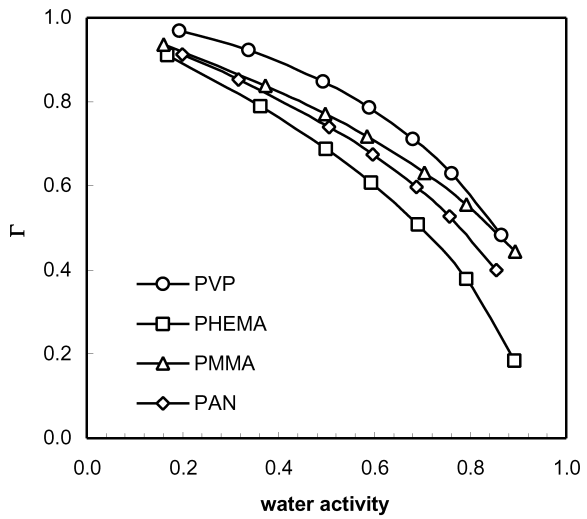

Fig. 9. Thermodynamic factor Γ versus water vapor activity for PVP, PHEMA, PMMA and PAN at 35 °C.

Although Γ is a decreasing function of solvent concentration for all four polymers, the measured diffusion coefficient increases significantly with rising water activity in PVP and PHEMA, slightly in PMMA; it is independent of concentration in PAN. Therefore, the concentration dependence of the diffusion coefficient cannot be explained in terms of a non-ideality factor and must be associated with an increase of the intrinsic mobility $Đ$ at higher activities. Plasticization of the polymer matrix induced by water sorption is likely responsible for the augmented intrinsic mobility upon increasing water concentration.

We have shown that water forms clusters in PHEMA, PMMA, and PAN. Water clustering is associated with a diffusion coefficient that decreases with rising solvent activity, whereas plasticization gives a diffusion coefficient that increases with solvent concentration [6,15]. Our results suggest that plasticization dominates at high activity, especially for PVP and PHEMA, whereas clustering and the concentration dependence of the thermodynamic factor cancel the effect of plasticization in PAN. Similar behavior has been observed for polyethersulfone [15] and for a series of polyarylates [6] with water as a penetrant.

4. Conclusions

Water vapor sorption and diffusion data at 35 °C have been obtained for four homopolymers of interest for packaging, insulation, and biomedical applications (such as drug-delivery systems) or for contact lens technology. Sorption results show that water has little solubility in PMMA and PAN, as expected for hydrophobic polymers. Water solubility is much higher in hydrophilic PVP and PHEMA. Data reduction using Flory–Huggins theory and the Zimm and Lundberg cluster integral shows that for polymers with strong interaction with water (PVP) water clustering is negligible, while for more hydrophobic polymers the degree of clustering appears to be larger.

Water diffusion is faster in PMMA than in PAN. In these two polymers, the diffusion coefficient is, respectively, weakly and not concentration dependent. For PVP and PHEMA, however, the diffusion coefficient is concentration-dependent and rises with increasing water vapor activity. Combined with the large upturn in the equilibrium isotherm, this trend suggests that the polymer matrix is plasticized by the solvent. Water diffusion is Fickian in PHEMA. The anomalous feature of sorption overshoot has been observed for PVP and PMMA at high water activity.

Acknowledgements

For financial support, the authors are grateful to the Office for Basic Sciences of the US Department of Energy and to the Donors of the Petroleum Research Fund, administered by the American Chemical Society; to

G. Ngao and D. Flaherty for help with the experimental work, and to L. Duda for helpful comments. O. Rodriguez and A. Arce thank the Ministerio de Ciencia y Tecnologia (Spain) for financial support through fellowships PN98-44807316 and FP2000-5251, respectively.

References

[1] Tighe B. Silicone hydrogels: how do they work? In: Sweeney D, editor. Silicone hydrogels: the rebirth of continuous wear contact lenses. Oxford: Butterworth-Heinemann; 2000. p. 1.
[2] Little SA, Bruce AS. ICLC 1995;22:148–55.
[3] Fonn D, Situ P, Simpson T. Optom Vis Sci 1999;76(10):700–4.
[4] Lebow K, Bridgewater B. ICLC 1997;24:198–206.
[5] Martellini F, Mei LHI, Balino JL, Carenza M. Radiat Phys Chem 2002;63(1):29–33.
[6] Kelkar AJ, Paul DR. J Membr Sci 2001;181(2):199–212.
[7] Rivin D, Kendrick CE, Gibson PW, Schneider NS. Polymer 2001; 42(2):623–35.
[8] de Queiroz AAA, Gallardo A. San Roman. J Biomaterials 2000; 21(16):1631–43.
[9] Hill DJT, Moss NG, Pomery PJ, Whittaker AK. Polymer 2000;41(4): 1287–96.
[10] Mantovani F, Grassi M, Colombo I, Lapasin R. Fluid Phase Equilib 2000;167(1):63–81.
[11] Striolo A, Prausnitz JM. Polymer 2000;41(3):1109–17.
[12] Zhang ZB, Britt IJ, Tung MA. J Polym Sci Pt B-Polym Phys 1999; 37(7):691–9.
[13] Chang MJ, Myerson AS, Kwei TK. J Appl Polym Sci 1997;66(2): 279–91.
[14] Del Nobile NA, Laurienzo P, Malinconico M, Mensitieri G, Nicolais L. Packaging Technol Sci 1997;10:95–108.
[15] Schult KA, Paul DR. J Polym Sci Pt B-Polym Phys 1996;34(16): 2805–17.
[16] Schult KA, Paul DR. J Polym Sci Pt B-Polym Phys 1997;35(6): 993–1007.
[17] Schult KA, Paul DR. J Polym Sci Pt B-Polym Phys 1997;35(4): 655–74.
[18] Schult KA, Paul DR. J Appl Polym Sci 1996;61(11):1865–76.
[19] Vrentas JS, Jarzebski CM, Duda JL. AICHE J 1975;21(5):894–901.
[20] Fujita H. Organic vapors above the glass transition temperature. In: Crank J, Park GS, editors. Diffusion in polymers. London: Academic Press; 1968. p. 75.
[21] Neogi P. Transport phenomena in polymer membranes. In: Neogi P, editor. Diffusion in polymers. New York: Marcel Dekker; 1996. p. 173.
[22] Gehrke SH, Biren D, Hopkins JJ. J Biomaterials Sci-Polym Ed 1994; 6(4):375–90.
[23] Fatt I. J Br Contact Lens Assoc 1989;12(2):15–31.
[24] Fornasiero F. Dissertation, University of California; in progress.
[25] Daubert TE, Danner RP. Physical and thermodynamic properties of pure chemicals: data compilation. New York: Hemisphere Publishing; 1989.
[26] Panayiotou C, Vera JH. Polym J 1984;16(2):89–102.
[27] Stannett VT, Ranade GR, Koros WJ. J Membr Sci 1982;10(2-3): 219–33.
[28] Katchman B, McLaren AD. J Am Chem Soc 1951;73(5):2124–7.
[29] Barrie JA. Water in polymer. In: Crank J, Park GS, editors. Diffusion in polymers. London: Academic Press; 1968. p. 259.
[30] Sun YM, Lee HL. Polymer 1996;37(17):3915–9.
[31] Fitzpatrick S, McCabe JF, Petts CR, Booth SW. Int J Pharm 2002; 246(1–2):143–51.
[32] Buera MD, Levi G, Karel M. Biotechnol Prog 1992;8(2):144–8.
[33] Oksanen CA, Zografi G. Pharm Res 1990;7(6):654–7.
[34] Fox TG. Bull Am Phys Soc 1956;1:123.
[35] Flory PJ. Principles of polymer chemistry. London: Cornell University Press; 1953.
[36] Rickles RN. Molecular Transport in Membranes, Industrial and Engineering Chemistry 1966;58(6):19.
[37] Rogers CE. In: Comyn J, editor. Polymer permeability. New York: Elsevier; 1985.
[38] Zimm BH, Lundberg JL. J Phys Chem 1956;60(4):425–8.
[39] Stannett V, Haider M, Koros WJ, Hopfenberg HB. Polym Engng Sci 1980;20(4):300–4.
[40] Ranade G, Stannett V, Koros WJ. J Appl Polym Sci 1980;25(10): 2179–86.
[41] Crank J. The mathematics of diffusion. Oxford: Clarendon Press; 1975.
[42] Overbergh N, Berghmans H, Smets G. Polymer 1975;16(10):703–8.
[43] Vittoria V. Polymer 1991;32(5):856–9.
[44] Alentiev A, Sanopoulou M, Ushakov N, Papadokostaki KG. Polymer 2002;43(6):1949–52.
[45] Etxeberria A, Etxabarren C, Iruin JJ. Macromolecules 2000;33(24): 9115–21.
[46] Ghi P, Hill DJT, Whittaker AK. J Polym Sci Pt B-Polym Phys 2000; 38(14):1939–46.
[47] Vrentas JS, Duda JL, Hou AC. J Appl Polym Sci 1984;29(1): 399–406.
[48] Hoyt MA, Balik CM. Polym Engng Sci 1996;36(14):1862–8.
[49] Kim DJ, Caruthers JM, Peppas NA. Macromolecules 1993;26(8): 1841–7.
[50] Aminabhavi TM, Phayde HTS. Polymer 1995;36(5):1023–33.
[51] Aminabhavi TM, Phayde HTS, Ortego JD. J Hazard Mater 1996; 46(1):71–88.
[52] Smith MJ, Peppas NA. Polymer 1985;26(4):569–74.
[53] Long FA, Richman D. J Am Chem Soc 1960;82(3):513–9.
[54] Ichikawa K, Mori T, Kitano H, Fukuda M, Mochizuki A, Tanaka M. J Polym Sci Pt B-Polym Phys 2001;39(18):2175–82.
[55] Taylor R, Krishna R. Multicomponent mass transfer. New York: Wiley; 1993.
[56] Kaplan H, Guner A. J Appl Polym Sci 2000;78(5):994–1000.